RESEARCH   Open Access

CrossMark

Antiapoptotic effects of scutellarin on ultraviolet A-irradiated HaCaT human keratinocytes

Mina Choi[1] and Seeun Jeon[2*]

Abstract

Background: This study examines the cellular protective effects of scutellarin on HaCaT cells in which oxidative stress was induced by ultraviolet A (UVA).

Methods: Cell viability and lipid peroxidation were measured using WST-1 and MDA assays, respectively. The changes in cell number in the sub-G1 phase were assessed using cell cycle analysis, and tailed DNA levels were measured using the comet assay to examine the degree of DNA damage. The difference in the mitochondrial membrane potential was examined using JC-1 staining, and the regulation of *BAX* mRNA expression levels was examined using quantitative real-time polymerase chain reaction.

Results: Although UVA-irradiated cells resulted in a 3.63-fold increase in lipid peroxide, scutellarin-treated cells showed concentration-dependent decreases of 2.06, 1.39, and 0.97 times at scutellarin concentrations of 1, 5, and 10 μM, respectively. The cell number in the sub-G1 phase increased by 227% when irradiated by UVA but decreased to 187, 139, and 120% when cells were treated with scutellarin at concentrations of 1, 5, and 10 μM, respectively. Tailed DNA also showed a protective effect. The mitochondrial membrane potential difference decreased up to 36% when irradiated by UVA but recovered up to 58, 82, and 92% when cells were treated with scutellarin at concentrations of 1, 5, and 10 μM, respectively. *BAX* gene expression levels increased 9.7-fold by UVA but was downregulated to 7.4-, 4.71-, and 2.49-fold when cells were treated with scutellarin at concentrations of 1, 5, and 10 μM, respectively.

Conclusions: This study revealed the cellular protective effects of scutellarin on HaCaT cells. Further studies are warranted to determine the use of scutellarin as a cosmeceutical ingredient.

Keywords: Scutellarin, Human keratinocytes, Ultraviolet A, Anti-apoptosis, Oxidative stress

Background

As an organic and complex organ that protects biological organs and has esthetic importance, the skin also reveals various aging mechanisms. Signs of skin aging include increasing wrinkles, loss in elasticity, pigmentation, and increasing white hair, among others (Appelqvist et al. 2013). Skin aging can be classified into two types: intrinsic aging, where the structure and physiological functions of skin deteriorate over time independent of the external environment, and photoaging, which is caused by sunlight. Among

the types of sunlight, ultraviolet is classified into three types based on wavelength (UVA 320–400 nm, UVB 280–320 nm, and UVC 200–280 nm), each with different reactions to skin. As the ozone layer in the stratosphere is consistently reduced by the pollutants in the air, the amount of ultraviolet radiation that reaches the earth increases. With the longest wavelength, UVA has an energy strength of 1/1000 of that of UVB but is expressed 20 times more frequently (Bernerd et al, 2011; Brugè et al, 2014; Chung 2003). It reaches indoor spaces through glass and deeply invades the dermis, epidermis, and subcutaneous fat layers. With the amount of light almost unvarying throughout the year, UVA uniformly irradiates the skin. In contrast to UVB, UVA rarely is absorbed by DNA, but it may damage DNA,

* Correspondence: jk35789@naver.com
[2]Management Division, Swinner, 5F, 441, Teheran-ro, Gangnam-gu, Seoul 06158, Republic of Korea
Full list of author information is available at the end of the article

membranes, and other cells, as well as induce cancer by generating reactive oxygen species (ROS) (Cross et al. 1987; Dimri et al. 1996). Recent studies on UVA verified the relationship between UVA and the harmful effects on carcinogenesis and immunosuppression (Fisher et al. 2002). As the outermost wall of the human body, skin is damaged by the primary invasion from the external environment to cause aging by oxidative stress from UVA (Gibbs et al. 2014; Giacomoni and Rein 2001). As skin is consistently exposed to ultraviolet rays, the accumulated UV promotes skin aging (Gruijl 2000). When exposed to excessive UV, mutations in DNA sequences inhibit the synthesis between the DNA structure and protein (Han et al. 2014). Damaged DNA delays the transcriptional activation of the *Bax* gene and the progression of the cell cycle (Haase et al. 2003). UVA and UVB cause apoptosis through different signaling pathways in HaCaT cells (Karran and Brem 2016). As they are most closely involved, they are among the subjects of interest in the field of esthetics (Marionnet et al. 2014). Oxidative stress from UVA and the products of photochemical reactions induce apoptosis in XP-A cells to induce skin aging and cancer (Oltvai et al. 1993). UV-induced apoptosis activates the cellular tumor antigen p53, while other features determine cell viability and apoptosis, including mitochondrial damages, cytochrome C release, caspase cascade activity through TNF-related apoptosis-inducing receptors, and the balance between apoptosis-inducing proteins such as Bax, Bak, Bid, and anti-apoptosis proteins such as Bcl-2, Bcl-xl, and Bcl-w (Ostling et al. 1984).

The epidermis acts as the moisturizing and defensive wall on the outermost layer of the skin. Comprising over 90% of the epidermis, keratinocytes play an important role in moisturization and skin rebuilding (O'Toole 2001; Podda and Grundmann-Kollmann 2001; Pustisek and Situm 2011; Rastogi et al. 2010). These keratinocytes create oxidative stress through its direct and consistent exposure to external irritants, such as UV and pollution (Sander et al. 2002). Chemokine, cytokine, and growth factors are secreted from the regions of skin damage by physical and chemical irritations to induce the proliferation and migration of keratinocytes. Such activities regenerate skin cells and strengthen the skin wall by promoting the proteins (including collagen) that comprise the skin.

Oxidative stress from oxygen free radicals influences almost every human disease. It is a major pathological factor in gene mutations and skin cell aging that deteriorates the normal functions of skin and induces various skin diseases, the functional deterioration of keratinocytes, inflammation, and necrosis of cells (Schultz and Wysocki 2009). Many researchers are studying substances that protect skin cells from such oxidative stress. Polyphenol compounds express antioxidant activity in combination with giant molecules. Flavonoids, a type of polyphenol compounds, prevent oxidization of lipids and eliminate oxygen free radicals to prevent aging.

Scutellarin, the subject of this study, is a type of flavonoid and an ingredient contained in skullcap (*Scutellaria indica* L.). Many previous studies have examined the protective effects of scutellarin against oxidative stress and apoptosis, but little attention has been paid to its effects on skin. This study examines the anti-apoptotic effects of scutellarin against oxidative stress induced by UVA in keratinocytes. In relation to the anti-apoptotic effects of scutellarin, this study examines the cell strains, loss in mitochondrial membrane potential difference, and changes in tailed DNA in HaCaT cells irradiated by UVA in the sub-G1 phase. In addition, this study examines whether *BAX* gene expression is regulated by scutellarin in human keratinocytes that are altered by UVA irradiation. The results reveal the anti-apoptotic effects of scutellarin on human keratinocytes altered by UVA and suggest the applicability of scutellarin as an anti-aging cosmetic ingredient.

Methods

Cell culture and sample treatment

HaCaT cells (ATCC, USA) were used as human keratinocytes for this experiment. For cell culture, DMEM (Hyclone, USA) was used as the medium, containing 10% fetal bovine serum (FBS; Hyclone) and 1% penicillin/streptomycin, cultured at 37 °C with 5% CO_2. Scutellarin (Sigma-Aldrich, USA) in powder form was dissolved in dimethyl sulfoxide (DMSO; Sigma-Aldrich) for the experiment. UVA was irradiated at 10 J/cm^2 through a UV-A lamp (UVP, USA).

Measuring the cell viability

The EZ-Cytox cell viability assay Kit (Itsbio, Korea) was used to test for cell toxicity of scutellarin. The WST-1 assay was used to measure the absorbance of formazan, generated by the dehydrogenase of the mitochondria. One hundred microliters of HaCaT cells (3×10^3 cells/ well) was divided into each well of a 96-well plate and cultured for 24 h. Scutellarin and UVA were treated in adequate concentrations and then cultured for 24 h. Ten microliters of the EZ-Cytox kit reagent was added to the cultured cells and then cultured for 1 h. Absorbance was measured at 450 nm using a microplate reader (Bio-Rad, USA). The experiment was repeated for three times to calculate the mean of cell viability.

mRNA extraction and cDNA synthesis

mRNA was extracted from the cultured cells using the Trizol reagent (Invitrogen, USA). The purity of the extracted mRNA was measured with a Nanodrop (Maestrogen, USA), and only mRNA with a 260/280 nm ratio of ≥ 1.8 was used in the experiments. cDNA was synthesized using M-MLV reverse transcriptase (Enzynomics, Korea) using 1 μg of RNA.

Quantitative real-time polymerase chain reaction

SYBR green (Invitrogen) was used to quantitatively analyze the patterns of gene expression in *BAX* mRNA caused by UVA and scutellarin in HaCaT cell. LineRNA K (BioER, China) was used to perform the polymerase chain reaction (PCR). The significance of the PCR results was verified with a melting curve. For each gene expression, *β-actin* was used as a standard for comparison. The primer sequences used for the experiment are shown in Table 1.

MDA assay

The malondialdehyde level was measured through colorimetry, while the lipid peroxidation (MDA) assay kit (Abcam, UK) was used to determine which peroxided lipid reacted with thiobarbituric acid (TBA) and was detected through colorimetry. HaCaT (1×10^6 cells/ml) cells were divided into a 96-well plate, where scutellarin was pre-processed at concentrations of 1, 5, and 10 μM and subsequently irradiated by UVA and then cultured for 24 h. The cells were homogenized in ice with MDA lysis buffer, and 200 μl of the supernatant was separated by centrifugation ($13,000 \times g$, 10 min). Six hundred microliters of TBA solution was poured into each test tube and then cooled to 95 °C for 1 h then in ice for 10 min for analysis in 96 wells by 200 μl. A microplate reader (Bio-Tek, USA) was used to measure absorbance at 586 nm.

Cell cycle analysis

A BD FACSCalibur flow cytometer (BD Biosciences, USA) was used to measure cell number in the sub-G1, G1, S, and G2/M phases to analyze the cell cycles. HaCaT cells (2×10^5 cells/well) were inoculated onto a 60-mm culture dish and then cultured for 24 h. Scutellarin at concentrations of 1, 5, and 10 μM was added and irradiated by UVA and then cultured for 24 h. The cultured cells were harvested, centrifuged for 5 min at 5000 rpm and 4 °C, and precipitated. Next, the supernatant was removed, and the cell pellet was suspended in 300 μl of PBS. While vortexing, 700 μl of absolute ethanol was added slowly and then stored at 4 °C for 3 h to immobilize the cells. One milliliter of PBS was added and centrifuged for 5 min at 5000 rpm at 4 °C to remove the supernatant. Two hundred microliters of the pellet was released in propidium iodide staining buffer (propidium iodide 50 μg/ml, RNase 0.1 μg/ml, 0.05% Triton X-100; all from Sigma-Aldrich) and incubated at 37 °C for 1 h. After centrifugation at 5000 rpm and 4 °C for 5 min to remove the supernatant

and a PBS wash, the pellet was released with 1 ml of PBS. Finally, the cell number was measured in each phase of the cell cycle with a flow cytometer.

Mitochondrial membrane potential assay

JC-1 (5,5′,6,6′-tetrachloro-1,1′,3,3′-tetraethylbenzimidazolylcarbocyanine iodide) mitochondrial membrane potential assay kit (Cayman chemical, USA) was used to perform an experiment on mitochondrial membrane potential to examine the effects of the sample on mitochondria. After cell seeding, samples were cultured for 24 h and then re-cultured for an additional 24 h after sample treatment and stimulus processing. Then, it was incubated at 37 °C for 20 min after adding JC-1, a fluorescent dye, and then washed twice in DPBS buffer (100 μl/ml of culture medium). Fluorescence was measured using a flow cytometer (red: excitation 550 nm, emission 600 nm/green: excitation 485 nm, emission 535 nm). The red/green fluorescence ratio was measured to determine mitochondrial depolarization.

Comet assay (single cell gel electrophoresis)

DNA tail was examined using a Comet assay reagent kit (Trevigen, USA) by measuring DNA damage. As a research method for studies on gene damage, the Comet assay was first introduced by Ostling and Johanson (Apoptosis 2009) to directly examine DNA damage across cellular levels. It uses electrophoresis, such that the migration rate is inversely proportional to the molecular mass. The analytical results show a comet-like shape through a microscope. LMAgarose was completely melted for 5 min, wrapped with a cap, and then sufficiently cooled in a water bath at 37 °C. LMAgarose (at 37 °C) was melted in 1×10^5 cell per milliliter cells and mixed at 1:10 (v/v), and 50 μl was placed on the comet slide at 4 °C for 10 min. The slide was immersed in an alkaline solution at room temperature. After the slide was placed and sealed in the alkaline electrophoresis solution, it underwent electrophoresis at 21 V for 30 min. After electrophoresis, it was immersed in distilled water twice for 4 min, and then, the electrophoresis solution was removed before being immersed in 70% ethanol for 5 min. It was dried at 37 °C for 15 min. The dry agarose gel was placed in 100 μl of SYBR Gold and then stained in a dark room for 30 min. Next, it was lightly rinsed in water to remove the remaining stain. The completely dried agarose gel at 37 °C was observed through a microscope.

Statistical analysis

All experiments for this study were repeated three times under the same conditions. The findings are expressed as mean ± standard deviation. Statistical significance was determined using a Student's t test, with significance values reported as follows: *$p < 0.05$, **$p < 0.01$, ***$p < 0.001$, #$p < 0.05$, ##$p < 0.01$, and ###$p < 0.001$.

Table 1 List of primers used in this study

Gene	Forward primer	Reverse primer
BAX	CCCTTTTCTACTTTGCCAGCAA	CCCGGAGGAAGTCCAATGT
B-actin	GGATTCCTATGTGGGCGACGA	CGCTCGGTGAGGATCTTCATG

Results

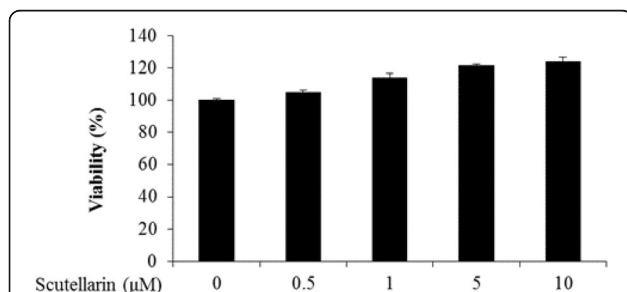## Protection of scutellarin against cell toxicity following UVA irradiation

To examine the cell toxicity of scutellarin in HaCaT cells, scutellarin was treated in HaCaT cells at concentrations of 0, 0.5, 1, 5, and 10 μM and cultured for 24 h and cell viability was measured using WST-1. No cell toxicity was detected at any of the concentrations (Fig. 1). On the other hand, HaCaT cells cultured in the presence of different concentrations of scutellarin following UVA irradiation showed cell viability of 61% in HaCaT cells in the UVA-irradiated group, in contrast to the non-treated control group. However, the cell viability varied in a concentration-dependent manner, with viabilities of 68, 75, 84, and 90% for concentrations of 0.5, 1, 5, and 10 μM, respectively (Fig. 2).

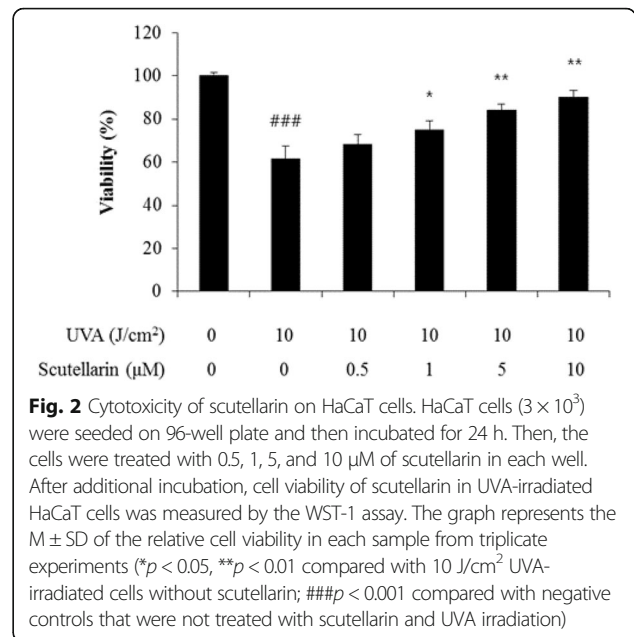## Changes in lipid peroxidation due to scutellarin in HaCaT cells irradiated with UVA

This experiment confirmed the inhibitive effect of scutellarin in intracellular lipid peroxidation induced by UVA. When HaCaT cells were irradiated by UVA (10 J/cm^2), lipid peroxidation increased 3.63 times more than that in the non-treated control group, whereas it decreased in a concentration-dependent manner, with values that were 2.06, 1.38, and 0.97 times greater due to increasing concentrations of scutellarin (1, 5, and 10 μM, respectively) (Fig. 3).

Changes in sub-G1 by scutellarin in HaCaT cells irradiated by UVA

The cell cycle was analyzed to examine how scutellarin protects cells from toxicity following UVA irradiation. HaCaT cells were stained with PI to measure the cell cycle progress with a flow cytometer. The changes caused by scutellarin in UVA-irradiated HaCaT cells in the sub-G1 phase were examined. When irradiated by UVA (10 J/cm^2), the

Fig. 2 Cytotoxicity of scutellarin on HaCaT cells. HaCaT cells (3×10^3) were seeded on 96-well plate and then incubated for 24 h. Then, the cells were treated with 0.5, 1, 5, and 10 μM of scutellarin in each well. After additional incubation, cell viability of scutellarin in UVA-irradiated HaCaT cells was measured by the WST-1 assay. The graph represents the M ± SD of the relative cell viability in each sample from triplicate experiments (*$p < 0.05$, **$p < 0.01$ compared with 10 J/cm^2 UVA-irradiated cells without scutellarin; ###$p < 0.001$ compared with negative controls that were not treated with scutellarin and UVA irradiation)

number of HaCaT cells increased in the sub-G1 phase by 228%, in contrast to the non-treated control group, but decreased by 188, 140, and 120%, in a concentration-dependent manner, in the experimental group treated by scutellarin in the concentrations of 1, 5, and 10 μM, respectively. Cell number and apoptosis increased due to UVA in the sub-G1 phase but decreased when cells were pre-processed with scutellarin to inhibit apoptosis. Scutellarin normalized the cell cycle to protect the cells (Fig. 4).
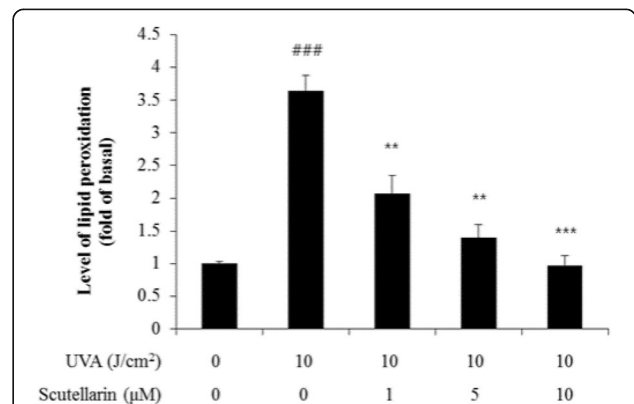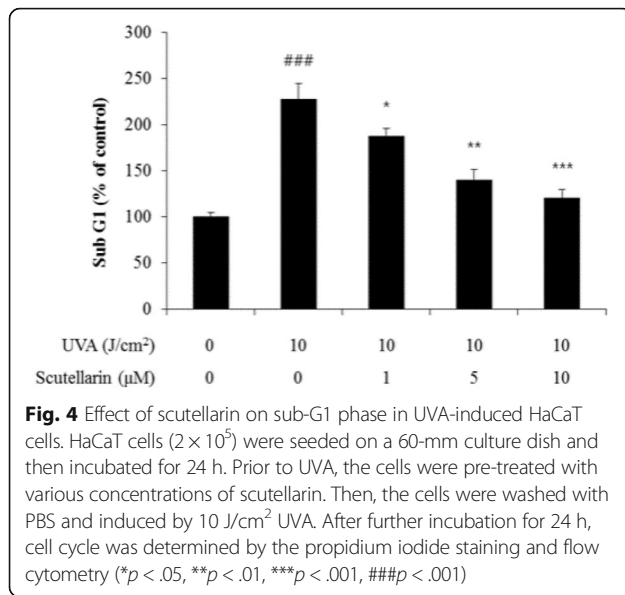

Fig. 1 Cytotoxicity of scutellarin on HaCaT cells. HaCaT cells (3×10^3) were seeded on a 96-well plate and then incubated for 24 h. Then, the cells were treated with 0.5, 1, 5, and 10 μM of scutellarin in each well. After additional incubation, cell viability of scutellarin in HaCaT cells was measured by the WST-1 assay. The graph represents the M ± SD of the relative cell viability in each sample from triplicate experiments

Fig. 3 Effect of scutellarin on UVA-induced lipid peroxidation in HaCaT cells. The lipid peroxidation analysis was examined by the lipid peroxidation (MDA) assay. Prior to UVA, the cells were pre-treated with various concentrations of scutellarin. HaCaT cells were homogenized on ice with the MDA lysis buffer and centrifuged ($13,000 \times g$, 10 min) to separate the supernatant (200 μl). The TBA solution (600 μl) was added to each test tube for 1 h at 95 ℃, and 10 min on ice, and dispensed in a 96-well by 200 μl for analysis. A microplate reader (Bio-Tek, USA) was used to measure in 586 nm. (**$p < .01$, ***$p < .001$, ###$p < .001$)

Fig. 4 Effect of scutellarin on sub-G1 phase in UVA-induced HaCaT cells. HaCaT cells (2×10^5) were seeded on a 60-mm culture dish and then incubated for 24 h. Prior to UVA, the cells were pre-treated with various concentrations of scutellarin. Then, the cells were washed with PBS and induced by 10 J/cm^2 UVA. After further incubation for 24 h, cell cycle was determined by the propidium iodide staining and flow cytometry ($*p < .05$, $**p < .01$, $***p < .001$, $###p < .001$)

Fig. 5 Effect of scutellarin on *Bax* mRNA in UVA-induced HaCaT cells. HaCaT cells (2×105) were cultured for 24 h after cell seeding and then used in experiments. In order to examine the protective effects of scutellarin against UVA, cells were pretreated with 1, 5, 10 μM of scutellarin and then the cells were washed with PBS followed by UVA irradiation. After further incubation for 24 h, the expression of BAX mRNA was determined by the qRT-PCR. The graph represents the mean ± SD of the relative expression level of BAX mRNA in each sample from triplicate experiments. ($**p < .01$, $***p < .001$, $###p < .001$)

### BAX mRNA expression regulation by scutellarin in UVA-irradiated HaCaT cells

The experiment confirmed that *Bax* mRNA was regulated by scutellarin in UVA-irradiated HaCaT cells. *Bax* reacts in the opposite way to *Bcl-2* to promote apoptosis (Wang et al. 2016). When irradiated by UVA (10 J/cm^2), the *BAX* mRNA expression was upregulated by 9.7 times relative to the non-treated control group, whereas it was downregulated by 7.4, 4.7, and 2.5 times in the experimental group treated across the various scutellarin concentrations (1, 5, and 10 μM) (Fig. 5). Scutellarin protected the cells by inhibiting apoptosis of keratinocytes through the intrinsic pathway.

Effect of scutellarin on mitochondrial membrane potential in UVA-irradiated HaCaT cells
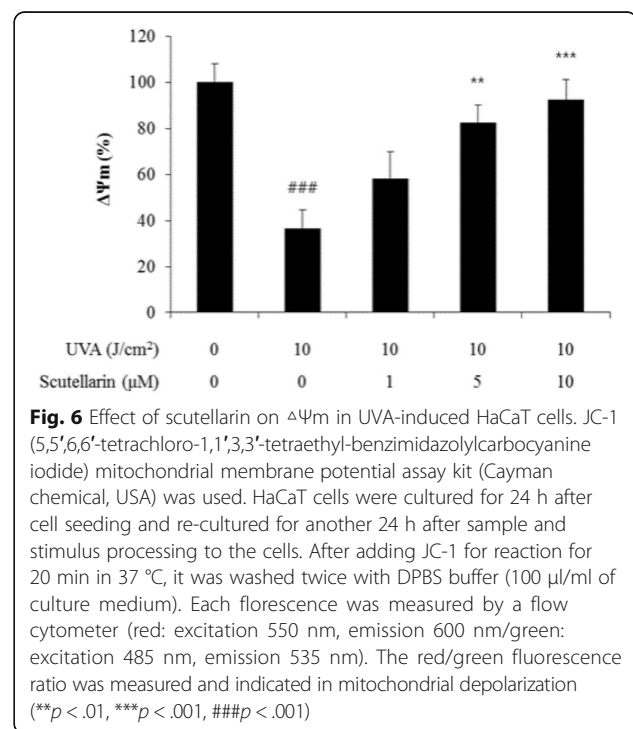
As a fluorescence stain, JC-1 is used for studies on mitochondrial membrane potential. It turns red in normal cells that generate J-aggregate but turns green in apoptotic cells due to the changes in membrane permeability, preventing the synthesis of ATP and lowering the concentration of JC-1 to exist in monomer. The changes in mitochondrial membrane potential ($\triangle \Psi m$) caused by scutellarin in UVA-irradiated HaCaT cells were examined. When irradiated by UVA (10 J/cm^2), $\triangle \Psi m$ decreased in HaCaT cells by 36%, in contrast to the non-treated control group. However, it increased in the experimental group treated with scutellarin at concentrations of 1, 5, and 10 μM by 58, 82, and 92%, in a concentration-dependent manner (Fig. 6).
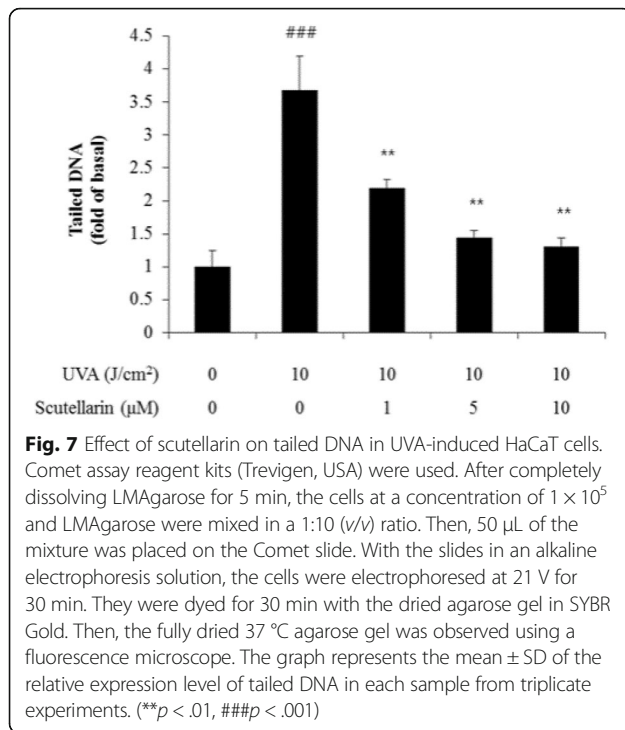
Changes in tailed DNA by scutellarin in UVA-irradiated HaCaT cells

The comet assay was used to measure intracellular DNA damage. When irradiated by UVA (10 J/cm^2), DNA tail in HaCaT cells increased 3.7 times relative
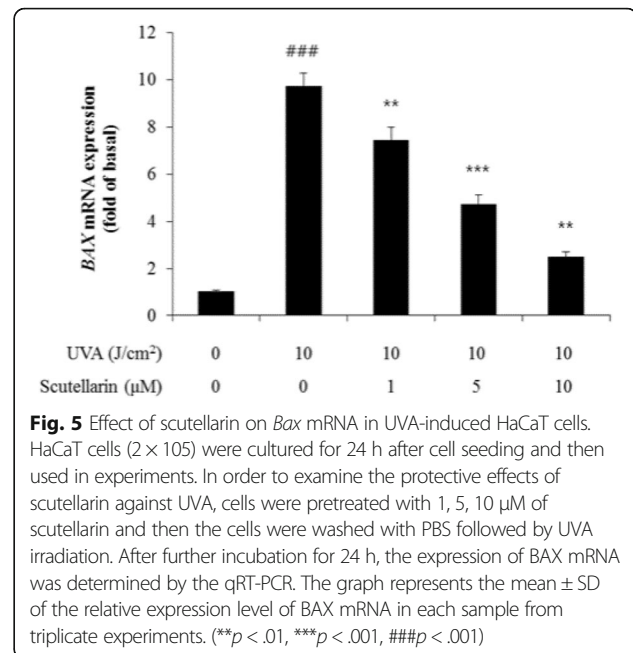
to the non-treated control group, presumably due to DNA damage by UVA irradiation. In the experimental group, where scutellarin was treated at concentrations of 1, 5, and 10 μM, DNA tail decreased by 2.2, 1.4, and 1.3 times, respectively. As a result, increased DNA damage due to UVA irradiation was protected by scutellarin, which inhibited damage (Fig. 7).

Fig. 6 Effect of scutellarin on $\triangle \Psi m$ in UVA-induced HaCaT cells. JC-1 (5,5′,6,6′-tetrachloro-1,1′,3,3′-tetraethyl-benzimidazolylcarbocyanine iodide) mitochondrial membrane potential assay kit (Cayman chemical, USA) was used. HaCaT cells were cultured for 24 h after cell seeding and re-cultured for another 24 h after sample and stimulus processing to the cells. After adding JC-1 for reaction for 20 min in 37 °C, it was washed twice with DPBS buffer (100 μl/ml of culture medium). Each florescence was measured by a flow cytometer (red: excitation 550 nm, emission 600 nm/green: excitation 485 nm, emission 535 nm). The red/green fluorescence ratio was measured and indicated in mitochondrial depolarization ($**p < .01$, $***p < .001$, $###p < .001$)

Fig. 7 Effect of scutellarin on tailed DNA in UVA-induced HaCaT cells. Comet assay reagent kits (Trevigen, USA) were used. After completely dissolving LMAgarose for 5 min, the cells at a concentration of 1×10^5 and LMAgarose were mixed in a 1:10 (v/v) ratio. Then, 50 µL of the mixture was placed on the Comet slide. With the slides in an alkaline electrophoresis solution, the cells were electrophoresed at 21 V for 30 min. They were dyed for 30 min with the dried agarose gel in SYBR Gold. Then, the fully dried 37 °C agarose gel was observed using a fluorescence microscope. The graph represents the mean ± SD of the relative expression level of tailed DNA in each sample from triplicate experiments. (**$p < .01$, ###$p < .001$)

Discussion

Scutellarin is reported to prevent ischemic heart disease-related damage by decreasing apoptosis and oxidative stress, inhibiting MDA production, causing mitochondrial membrane potential (MMP) loss, and increasing Bax gene expression in damaged cardiomyocytes (Wang et al. 2016). Harmful reactive oxygen species are naturally produced in vivo as a byproduct of oxygen consumption. In addition to ultraviolet (UV) rays, external and internal environmental factors disturb the balance of reactive oxygen species, and a chain reaction caused by excess levels of reactive oxygen species facilitates aging, skin thickening, wrinkle formation, and inflammation, which lead to a variety of skin diseases (Bickers and Athar 2006; Campisi 1998). In HaCaT, UVA increases oxidative stress by decreasing glutathione (GSH) levels (Assefa et al. 2005), which leads to DNA cleavage and damage, chromosomal anomalies, and carcinogenesis (Wischermann et al. 2008). Skin is susceptible to oxidative stress because it is frequently exposed to UV rays and has a high content of lipids, which are extremely vulnerable to attacks by reactive oxygen species. Lipids destroyed by UV exposure are highly reactive and have toxicity similar to that of reactive oxygen species, and these lipid peroxides attack and damage cells. To examine the antioxidant activity of scutellarin in UVA-irradiated HaCaT cells, a lipid peroxidation test was performed, and it showed that scutellarin has an antioxidant activity. When apoptosis (which is different from necrosis) occurs, double helical DNA in the nucleus is cleaved at the junctions between nucleosomes, generating truncated fragments of 180–200 base pairs (Vaux 1993).

DNA cleavage between nucleosomes is regulated by enzymes, such as Ca/Mg-dependent restriction enzymes, deoxyribonuclease II, and Mg-dependent restriction enzymes (Counis and Torriglia 2000). Diseases caused by the abnormal suppression of apoptosis include cancers, autoimmune diseases, and viral infections, whereas diseases caused by the abnormal increase of apoptosis include acquired immune deficiency syndrome (AIDS), Alzheimer's disease, myelodysplastic syndrome, and ischemia-related diseases (Carson). Apoptosis progression in cells is dependent on the extent of cellular damage, intracellular calcium levels, and intracellular adenosine triphosphate (ATP) levels (Eguchi et al. 1997). Bcl-2 family genes are divided into an anti-apoptosis group, including Bcl-2 and Bcl-xl, which suppress cytochrome C release through a protein complex located in the mitochondrial outer membrane, and a pro-apoptosis group, including Bax, Bad, and Bid. The latter move into the mitochondria and induce cytochrome C release following the death signal. As apoptosis progresses, there is an increase in the number of sub-G1 phase cells, which are typically absent, and the number of DNA tails increases because of damaged DNA fragments, leading to the loss of mitochondrial membrane potential (MMP) difference. Scutellarin decreases the viability of human colon cancer cells and induces apoptosis by controlling the mRNA expression of p53, Bcl-2, and Bax (Yang et al. 2017). After irradiating HaCaT cells with 10 mJ/cm² of UVA, the transcriptional regulation of Bax mRNA was examined by qRT-PCR. Although the level of Bax mRNA rapidly increased, it decreased in a concentration-dependent manner in the scutellarin-treated group. In addition, when human colorectal cells were treated with *Scutellaria barbata* extracts containing scutellarin and analyzed by flow cytometry, the number of sub-G1 phase cells was significantly increased at higher concentrations of the extracts in a concentration-dependent manner, indicating that scutellarin induces apoptosis in human colon cancer cells (Goh et al. 2005). The outer membrane of the mitochondria allows large molecules to be embedded in the intermembrane space, whereas the inner membrane is responsible for oxidative phosphorylation. During oxidative phosphorylation, protons are released from the mitochondrial matrix into the intermembrane space, producing an electrochemical gradient called MMP (Evenson et al. 1982). If the mitochondria are exposed to reactive oxygen species, membrane permeability is changed to form permeation transition pores (Bernardi et al. 1994). When these pores are opened, cytochrome C is released from the mitochondria and acts as a cell death signal. In addition, due to the loss of MMP, ATP cannot be synthesized and the intracellular Ca^{2+} level increases, leading to apoptosis (Zaidan and Sims 1994). MMP difference was observed using JC-1, a fluorescent dye. JC-1 is present as a monomer at low concentrations, when it displays green fluorescence. At high concentrations, it forms J-aggregates

that display red fluorescence. Therefore, when mitochondria with high membrane potentials are observed under a fluorescence microscope, JC-1 fluorescence changes from green to red. The effect of scutellarin on changes in the MMP was investigated in HaCaT cells using JC-1. This showed that UVA irradiation decreased the mitochondrial membrane potential, inducing apoptosis. However, in the scutellarin-pretreatment group, the membrane potential was rescued sufficiently to prevent MMP loss. This demonstrates that scutellarin has a protective effect against oxidative stress-related apoptosis.

Conclusions

This study examined the cellular protective effects of scutellarin in keratinocytes damaged by UVA. No cell toxicity of scutellarin was observed in keratinocytes, but UVA affected keratinocytes and increased lipid peroxidation. Scutellarin inhibited and gradually decreased lipid peroxidation. In addition, the cell number was reduced in the sub-G1 phase, which has been discovered rarely in a normal cell cycle. In HaCaT cells pre-processed with scutellarin, *Bax* mRNA expression decreased to promote apoptosis. Finally, scutellarin protected DNA from damage and decreased loss in mitochondrial membrane potential difference due to UVA irradiation. As a consequence of these protective effects for the skin, scutellarin is a potentially applicable ingredient for anti-aging cosmetics to protect skin damage from UVA. Additional studies are needed to verify various effects of scutellarin for its commercialization.

Abbreviations
$\triangle\Psi$m: Mitochondrial membrane potential; BAX: Bcl-2-associated X protein; DMEM: Dulbecco's modified Eagle's medium; DMSO: Dimethyl sulfoxide; FBS: Fetal bovine serum; JC-1: 5,5',6,6'-tetrachloro-1,1',3,3'-tetraethylbenzimidazolylcarbocyanine iodide; MDA: Malondialdehyde; PBS: Phosphate-buffered saline; PI: Propidium iodide; qRT-PCR: Quantitative real-time polymerase chain reaction; ROS: Reactive oxygen species; TBA: Thiobarbituric acid; TNF: Tumor necrosis factor; WST: Water soluble tetrazolium salt; β-actin: Actin beta

Availability of data and materials
Not applicable.

Authors' contributions
SJ did the research background such as the experiments, data collection, and statistical analysis, and MC wrote the manuscript draft. All authors read and approved the final manuscript.

Ethics approval and consent to participate
Not applicable.

Consent for publication
Not applicable.

Competing interests
The authors declare that they have no competing interests.

Publisher's Note
Springer Nature remains neutral with regard to jurisdictional claims in published maps and institutional affiliations.

Author details
[1]Department of Liberal Arts, Jangan University, Samcheonbyeongma-ro, Bongdam-eup, Hwaseong-si, Gyeonggi-do 18331, Republic of Korea. [2]Management Division, Swinner, 5F, 441, Teheran-ro, Gangnam-gu, Seoul 06158, Republic of Korea.

References
Tomas D. Apoptosis, UV-radiation, precancerosis and skin tumors. Acta Med Croatica. 2009;63:53–8.

Appelqvist H, Wäster P, Eriksson I, Rosdahl I, Ollinger K. Lysosomal exocytosis and caspase-8-mediated apoptosis in UVA-irradiated keratinocytes. J Cell Sci. 2013;126:5578–84.

Assefa Z, Van Laethem A, Garmyn M, Agostinis P. Ultraviolet radiation-induced apoptosis in keratinocytes: on the role of cytosolic factors. Biochim Biophys Acta. 2005;1755:90–106.

Bernardi P, Broekemeier KM, Pfeiffer DR. Recent progress on regulation of the mitochondrial permeability transition pore; a cyclosporin-sensitive pore in the inner mitochondrial membrane. J Bioenerg Biomembr. 1994;26:509–17.

Bernerd F, Del Bino S, Asselineau D. Regulation of keratin expression by ultraviolet radiation: differential and specific effects of ultraviolet B and ultraviolet a exposure. J Investig Dermatol. 2011;117:1421–9.

Bickers DR, Athar M. Oxidative stress in the pathogenesis of skin disease. J Invest Dermatol. 2006;126:2565–75.

Brugè F, Tiano L, Astolfi P, Emanuelli M, Damiani E. Prevention of UVA-induced oxidative damage in human dermal fibroblasts by new UV filters, assessed using a novel in vitro experimental system. PLoS One. 2014;9:e83401.

Campisi J. The role of cellular senescence in skin aging. J Investig Dermatol Symp Proc. 1998;3:1–5.

Chung JH. Photoaging in Asians. Photodermatol Photoimmunol Photomed. 2003; 19:109–21.

Counis MF, Torriglia A. DNases and apoptosis. Biochem Cell Biol. 2000;78:405–14.

Cross CE, Halliwell B, Borish ET, Pryor WA, Ames BN, Saul RL, McCord JM, Harman D. Oxygen radicals and human disease. Ann Intern Med. 1987;107:526–45.

Dimri GP, Testori A, Acosta M, Campisi J. Replicative senescence, aging and growth-regulatory transcription factors. Biol Signals. 1996;5:154–62.

Eguchi Y, Shimizu S, Tsujimoto Y. Intracellular ATP levels determine cell death fate by apoptosis or necrosis. Cancer Res. 1997;57:1835–40.

Evenson DP, Darzynkiewicz Z, Melamed MR. Simultaneous measurement by flow cytometry of sperm cell viability and mitochondrial membrane potential related to cell motility. J Histochem Cytochem. 1982;30:279–80.

Fisher GJ, Kang S, Varani J, Bata-Csorgo Z, Wan Y, Datta S, Voorhees JJ. Mechanisms of photoaging and chronological skin aging. Arch Dermatol. 2002;138:1462–70.

Giacomoni PU, Rein G. Factors of skin ageing share common mechanisms. Biogerontology. 2001;2:219–29.

Gibbs S, Backendorf C, Ponec M. Regulation of keratinocyte proliferation and differentiation by all-trans-retinoic acid, 9-cis-retinoic acid and 1,25-dihydroxy vitamin D3. Arch Dermatol Res. 2014;288:729–38.

Goh D, Lee YH, Ong ES. Inhibitory effects of a chemically standardized extract from Scutellaria barbata in human colon cancer cell lines, LoVo. J Agric Food Chem. 2005;53:8197–204.

Gruijl FR. Photocarcinogenesis: UVA vs UVB. Methods Enzymol. 2000;319:359–66.

Haase I, Evans R, Pofahl R, Watt FM. Regulation of keratinocyte shape, migration and wound epithelialization by IGF-1- and EGF-dependent signalling pathways. J Cell Sci. 2003;116(Pt 15):3227–38.

Han A, Chien AL, Kang S. Photoaging. Dermatol Clin. 2014;32:291–9.

Karran P, Brem R. Protein oxidation, UVA and human DNA repair. DNA Repair (Amst). 2016;44:178–85.

Marionnet C, Pierrard C, Golebiewski C, Bernerd F. Diversity of biological effects induced by longwave UVA rays (UVA1) in reconstructed skin. PLoS One. 2014;9:e105263.

Oltvai ZN, Milliman CL, Korsmeyer SJ. Bcl-2 heterodimerizes in vivo with a conserved homolog, Bax, that accelerates programmed cell death. Cell. 1993;74:609–19.

Ostling O, Johanson KJ, et al. Biochem Biophys Res Commun. 1984;123:291–8.

O'Toole EA. Extracellular matrix and keratinocyte migration. Clin Exp Dermatol. 2001;26:525–30.

Podda M, Grundmann-Kollmann M. Low molecular weight antioxidants and their role in skin ageing. Clin Exp Dermatol. 2001;26:578–82.

Pustisek N, Situm M. UV-radiation, apoptosis and skin. Collegium Antropologicum. 2011;35:339–41.

Rastogi RP, Richa, Kumar A, Tyagi MB, Sinha RP. Molecular mechanisms of ultraviolet radiation-induced DNA damage and repair. Journal of Nucleic Acids. 2010;32:e592980.

Sander CS, Chang H, Salzmann S, Müller CS, Ekanayake-Mudiyanselage S, Elsner P, Thiele JJ. Photoaging is associated with protein oxidation in human skin in vivo. J Invest Dermatol. 2002;118:618–25.

Schultz GS, Wysocki A. Interactions between extracellular matrix and growth factors in wound healing. Wound Repair Regen. 2009;17:153–62.

Vaux DL. Toward an understanding of the molecular mechanisms of physiological cell death. Proc Natl Acad Sci U S A. 1993;90:786–9.

Wang Z, Yu J, Wu J, Qi F, Wang H, Wang Z, Xu Z. Scutellarin protects cardiomyocyte ischemia-reperfusion injury by reducing apoptosis and oxidative stress. Life Sci. 2016;157:200–7.

Wischermann K, Popp S, Moshir S, Scharfetter-Kochanek K, Wlaschek M, de Gruijl F, Hartschuh W, Greinert R, Volkmer B, Faust A, Rapp A, Schmezer P, Boukamp P. UVA radiation causes DNA strand breaks, chromosomal aberrations and tumorigenic transformation in HaCaT skin keratinocytes. Oncogene. 2008;27:4269–80.

Yang N, Zhao Y, Wang Z, Liu Y, Zhang Y. Scutellarin suppresses growth and causes apoptosis of human colorectal cancer cells by regulating the p53 pathway. Mol Med Rep. 2017;15:929–35.

Zaidan E, Sims NR. The calcium content of mitochondria from brain subregions following short-term forebrain ischemia and recirculation in the rat. J Neurochem. 1994;63:1812–9.